“Cooperative Diversity for Free Space Optical Communication: Transceiver Design & Performance Analysis”

By:
Ahmad Slim

Advisor:
Dr. Chadi Abou Rjeily

Department of Electrical & Computer Engineering

To My Parents

Abstract

In this work, we investigate the cooperative diversity technique as a candidate solution for combating turbulence-induced fading over Free-Space Optical (FSO) links. In particular, a one-relay cooperative diversity scheme is proposed and analyzed for non-coherent FSO communications with intensity modulation and direct detection (IM/DD). The error performance of this diversity scheme is derived in semi-analytical and closed-form expressions in the presence and absence of background radiation, respectively. Results show the enhanced diversity orders that can be achieved over both Rayleigh and lognormal fading models.

Table of Contents

List of Figures

List of Tables

I. Introduction

Recently, Free-Space Optical (FSO) communications attracted significant attention as a promising solution for the “last mile” problem [1]. A major impairment that severely degrades the link performance is fading (or scintillation) that results from the variations of the index of refraction due to inhomogeneities in temperature and pressure changes [2]. In order to maintain acceptable performance levels over FSO links, fading-mitigation techniques such as spatial diversity techniques must be employed. Spatial diversity involves the deployment of multiple transmit and/or receiver apertures and is commonly used to combat fading and improve the link reliability as shown in Fig.1.

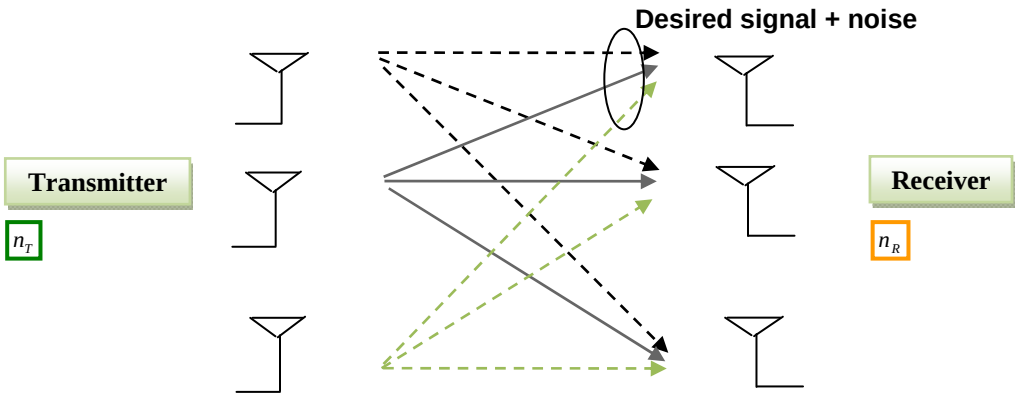

Figure 1: Atmospheric optical MIMO system model.

Diversity combining techniques were extensively studied in the context of radio-frequency (RF) wireless transmissions and were recently extended and tailored to FSO transmissions. In this context, aperture-averaging receiver diversity [3], spatial repetition codes [4], unipolar versions of the orthogonal space-time codes [5] and transmit laser selection [6] were proposed as FSO adapted spatial diversity solutions. In the same way, the bit error rates of Multiple-Input-Multiple-Output (MIMO) FSO links were evaluated in [7] and [8].

On the other hand, in RF systems cooperative diversity techniques are becoming more popular in situations where limited number of antennas can be deployed at the mobile terminals [9], [10]. In this context, neighboring nodes can form “virtual” antenna

arrays and profit from the underlying spatial diversity in a distributed manner. Cooperative diversity takes advantage of the broadcast nature of RF transmissions where a message transmitted from a source to a destination can be overheard by neighboring nodes. If these nodes are willing to cooperate with the source, they retransmit information about the same message to the destination thus enhancing the quality of signal reception. Despite the extensive research in RF wireless cooperation, to the author's best knowledge, this technique was never considered before in the context of FSO communications.

In this work, we investigate for the first time the utility of cooperative diversity as a means of combating fading in FSO links. In particular, we consider a decode-and-forward strategy with one relay over FSO links with intensity modulation and direct detection (IM/DD). The main reason that discourages the investigation of cooperation in FSO systems resides in the non-broadcast nature of optical transmissions. In FSO, the source can not broadcast an information message to the destination and to a distant relay simultaneously. Consequently, an additional transmit power must be entirely dedicated for delivering the message to the relay. None of this power will reach the destination implying an additional power penalty (as compared to RF wireless cooperation). However, this work shows that the cooperative diversity can be useful in enhancing the performance of FSO links since the gain in diversity can compensate for this power penalty.

On the other hand, the factors encouraging the implementation of the cooperative diversity technique are as follows. (1): The solution is cost-effective (compared to MIMO-FSO) since it does not require adding more apertures to the transmitter and/or receiver. (2): It is well known that channel correlation degrades the performance of MIMO systems whether in FSO or RF scenarios. However, MIMO-FSO channels are more likely to be correlated. In fact, in RF systems the signal reaches the receiver by a large number of paths implying that a small separation between the antennas can ensure channel independence. On the other hand, FSO links are much more directive thus rendering the path gains between the transmit and receive elements more dependent; for example, the presence of a small cloud between the transmitter and receiver as shown in Fig.2 can induce large fades on all source-detector pairs simultaneously [4].

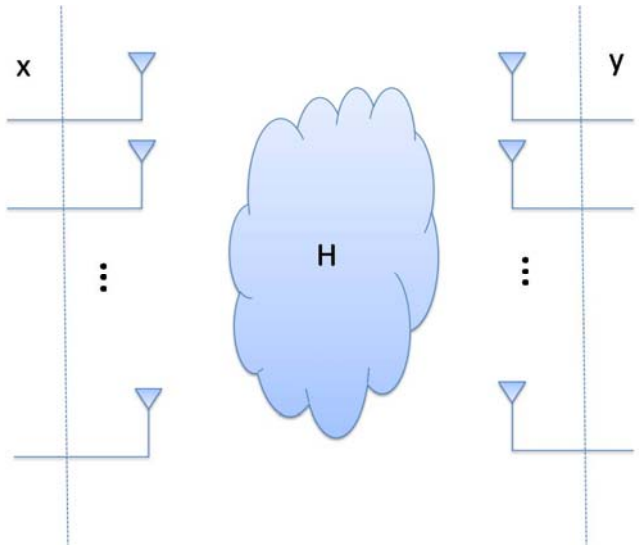

Figure 2: Large fades induced by a cloud existing between the transmitters and receivers.

Consequently, the high performance gains promised by MIMO-FSO solutions under the assumption of channel independence [4]–[6] might not be achieved in practice. Consequently, as stated in [4] "*alternative means of operation in such environments must be considered*". In this context, cooperation can constitute a good candidate alternative. In fact, given the large distances (in the order of kilometers) between the source-destination, source-relay and relay-destination, the assumption of independence is more valid compared to the case of co-located arrays. (3): Unlike RF systems, extending the MIMO techniques to FSO systems imposes a compromise on the choice of the sources. The sources must be narrow enough to couple more power from the transmitter to the receiver and they must be wide enough to illuminate all detectors simultaneously. Consequently, the wider spacing of detectors (necessary for channel independence) results in an increased transmit power.

In this context, taking advantage of the spatial diversity in a distributed manner by deploying the proposed cooperative scheme permits to overcome this limitation and can constitute a good practical alternative to MIMO-FSO systems.

II. System Model And Transmitter Structure

Consider the example of a FSO Metropolitan Area Network as shown in Fig. 3.

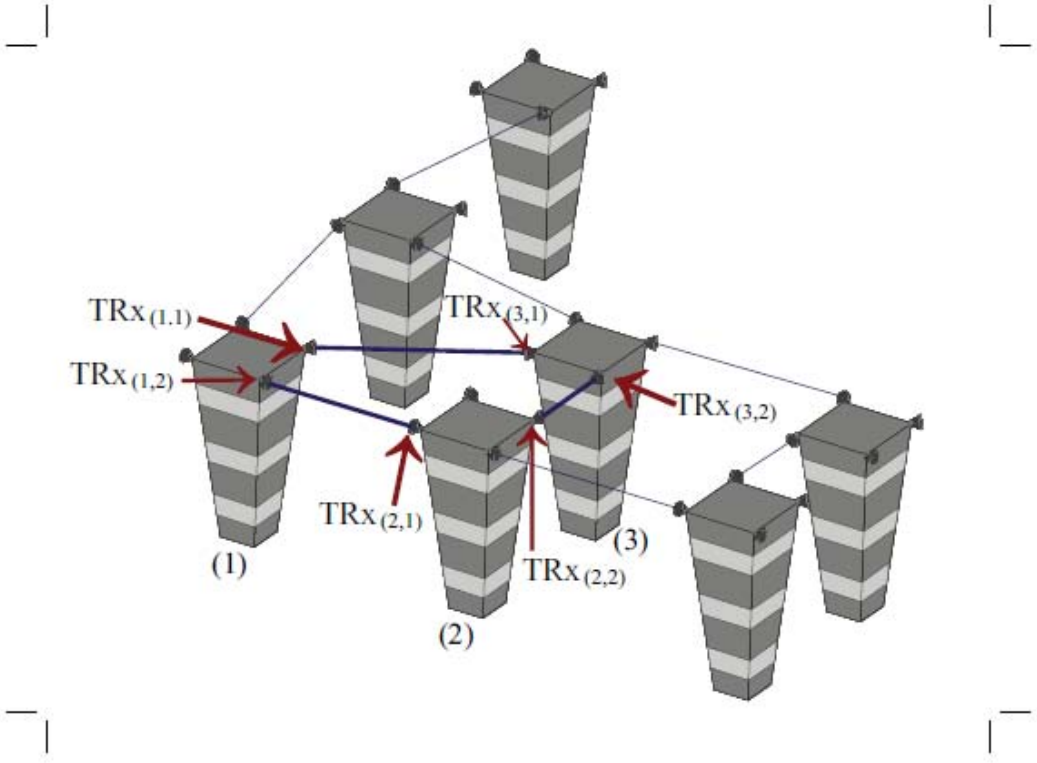

Figure 3: An example of a mesh FSO network. Cooperation is proposed among the transceivers on buildings (1), (2) and (3) where the transceivers on building 2 can help in transmitting an information message from (1) to (3). Note how, given the non-broadcast nature of FSO transmissions, one couple of FSO transceiver units is dedicated for each link.

Consider three neighboring buildings (1), (2) and (3) and assume that a FSO connection is available between each building and its two neighboring buildings. In FSO networks, each one of these connections is established via FSO-based wireless units each consisting of an optical transceiver -shown in Fig. 4- with a transmitter and a receiver to provide full-duplex capability.

Figure 4: An 8-beam free space optics laser link. The receiver is the large disc in the middle, the transmitters the smaller ones.To the top and right side a monocular for assisting the alignment of the two heads

Given the high directivity and non-broadcast nature of FSO transmissions, one separate transceiver is entirely dedicated for the communication with each neighboring building. We assume that the transceivers on building (2) are available for cooperation to enhance the communication reliability between buildings (1) and (3). By abuse of notations, buildings (1), (2) and (3) will be denoted by source (S), relay (R) and destination (D), respectively. The cooperation strategy is depicted in Fig. 5.

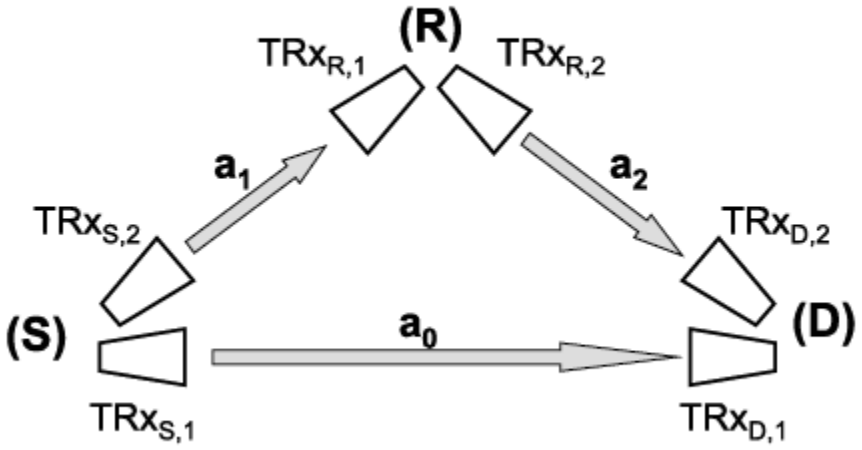

Figure 5: The proposed cooperation scheme.

It is worth noting that the transceivers at (R) are not deployed with the objective of assisting (S). In fact, these transceivers are deployed for (R) to communicate with (S) and (D); if (R) is willing to share its existing resources (and (R) has no information to transmit), then it can act as a relay for assisting (S) in its communication with (D). The cooperation strategy is as follows: a sequence of symbols is first transmitted to the relay. At a second time, (R) transmits the decoded symbols to (D) while (S) transmits the same symbol sequence simultaneously to (D). Since three transmissions are involved in each cooperation cycle, then the transmitted power from transceivers $TRx_{S,1}$, $TRx_{S,2}$ and $TRx_{R,2}$ must be divided by 3.

Denote by a_0, a_1 and a_2 the random path gains between S-D, S-R and R-D, respectively. In this work, we adopt the lognormal and Rayleigh turbulence-induced fading channel models [4]. In the lognormal model, the probability density function (pdf) of the path gain ($a > 0$) is given by: $f_A(a) = \frac{1}{\sqrt{2\pi}\sigma a}\exp\left(-\frac{(\ln a - \mu)^2}{2\sigma^2}\right)$ where the parameters μ and σ satisfy the relation $\mu = -\sigma^2$ so that the mean path intensity is unity: $E[I] = E[A^2] = 1$. The degree of fading is measured by the scintillation index defined by:

S.I. = $e^{4\sigma^2} - 1$. Typical values of S.I. range between 0.4 and 1. In the Rayleigh model, the pdf of the path gain (a > 0) is: $f_A(a) = 2ae^{-a^2}$.

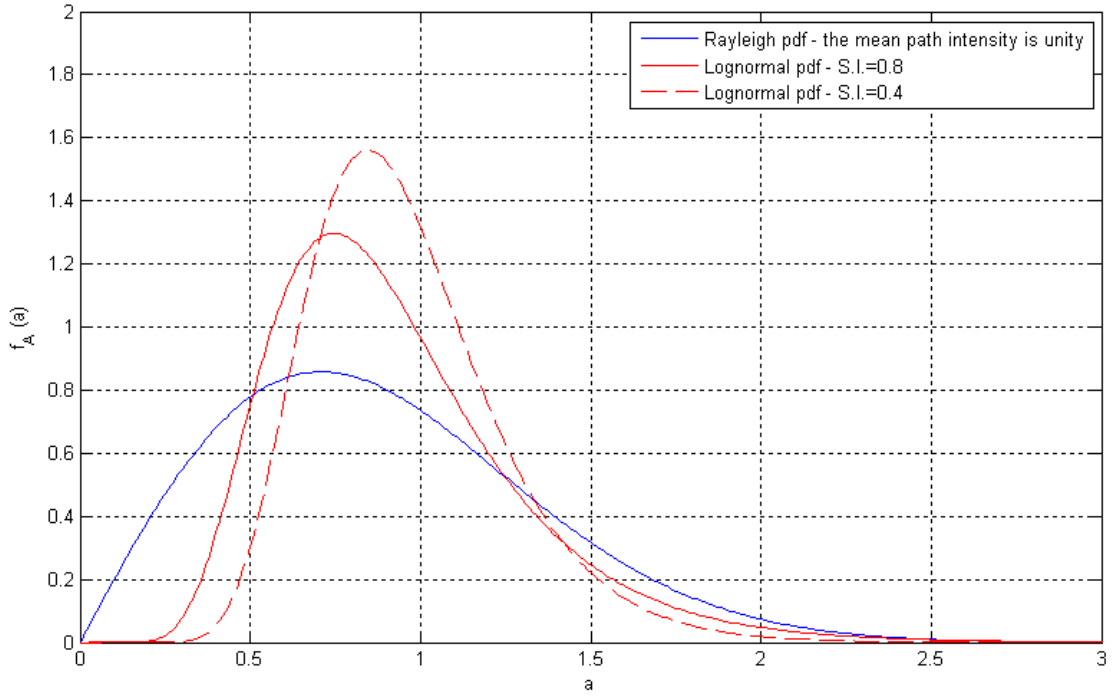

Figure 6: Log-normal and Rayleigh pdfs

Fig. 6 shows the probability density functions of both Rayleigh and Log-normal fading. In particular two values for the scintillation index (S.I.) were taken for the Log-normal case. Analyzing the pdfs, it would be clear that low values of 'a' have a higher density in the Rayleigh case than that of the Log-normal case and this certainly imposes more fading on the system performance.

Consider Q-ary pulse position modulation (PPM), shown in Fig. 7, with IM/DD links where the receiver corresponds to a photoelectrons counter. Consider first the link S-D and denote by $Z^{(0)} = \left[Z_1^{(0)}, \ldots, Z_Q^{(0)}\right]$ the Q-dimensional vector whose *q*-th component $Z_q^{(0)}$ corresponds to the number of photoelectron counts in the *q*-th slot.

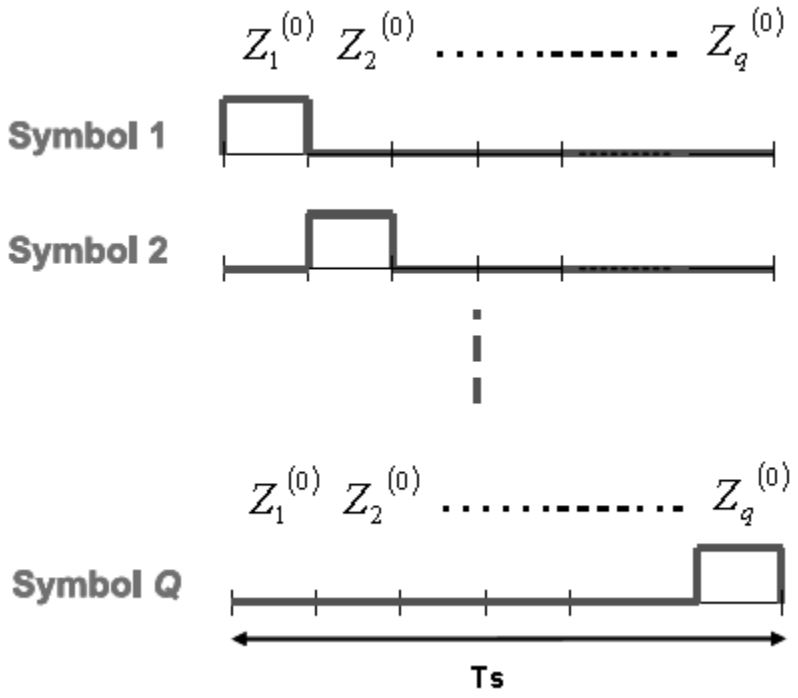

Figure 7: Q-ary pulse position modulation (PPM)

Denote the transmitted symbol by $s \in \{1, \ldots, Q\}$. The decision variable $Z_s^{(0)}$ can be modeled as a Poisson random variable (r.v.), shown in Fig. 8, with parameter $a_0^2 \lambda_s / 3 + \lambda_n$ while $Z_q^{(0)}$ (with $q \neq s$) can be modeled as a Poisson r.v. with parameter λ_n [4]:

$$\Pr\left(Z_q^{(0)} = K\right) = \begin{cases} e^{-\left(a_0^2 \lambda_s / 3 + \lambda_n\right)} \left(a_0^2 \lambda_s / 3 + \lambda_n\right)^k, & q = s; \\ \dfrac{e^{-\lambda_n} \lambda_n^{\,k}}{k!}, & q \neq s. \end{cases} \qquad (1)$$

where λ_s (resp. λ_n) corresponds to the average number of photoelectrons per slot due to the light signal (resp. background radiation and "dark currents"):

$$\lambda_s = \eta \frac{P_r T_s / Q}{hf} = \eta \frac{E_s}{hf} \quad ; \quad \lambda_n = \eta \frac{P_b T_s / Q}{hf} \qquad (2)$$

where η is the detector's quantum efficiency assumed to be equal to 1 in what follows, $h = 6.6 \times 10^{-34}$ is Planck's constant and f is the optical center frequency taken to be 1.94×10^{14} (corresponding to a wavelength of 1550 nm). T_s stands for the symbol duration, P_r stands for the optical power that is incident on the receiver and P_b corresponds to the incident background power. Finally, $E_s = P_r T_s / Q$ corresponds to the received optical energy per symbol corresponding to the direct link S-D. Readers can refer to [4] for more details on the system model.

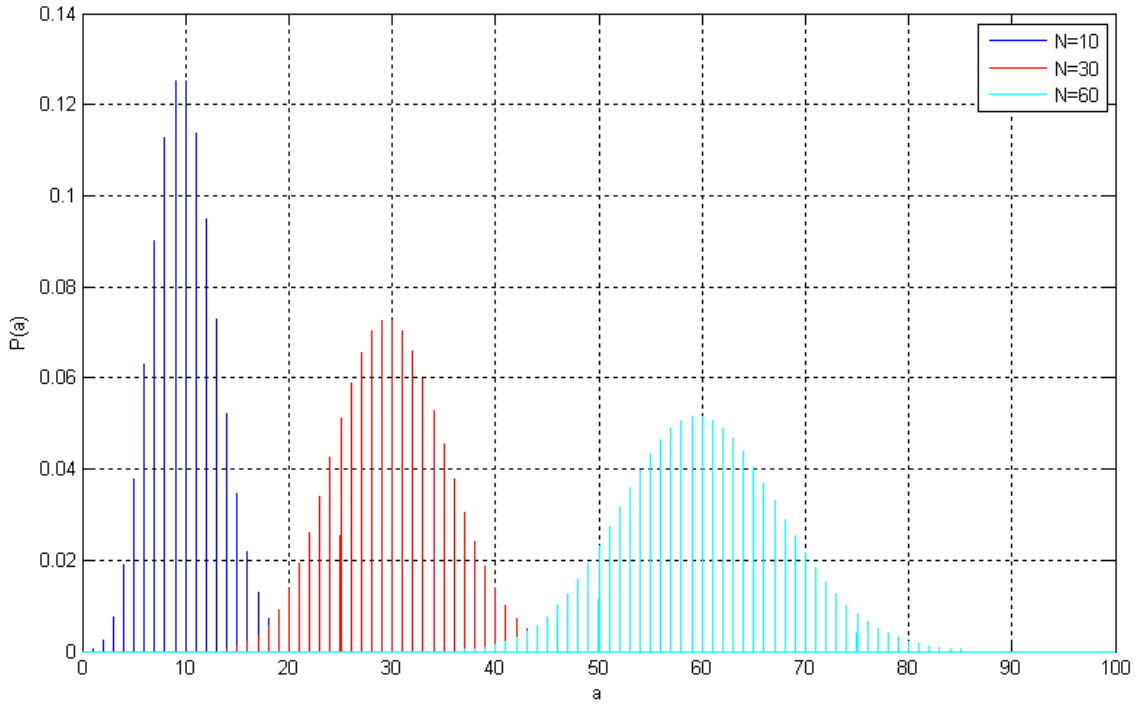

Figure 8: Poisson distribution with three values of N where N is the expected number of photoelectrons

In the same way, we denote the decision vector corresponding to the S-R link by $Z^{(1)} = \left[Z_1^{(1)}, \ldots, Z_Q^{(1)} \right]$ where the parameter of the Poisson r.v. $Z_q^{(1)}$ is given by:

$$E\left[Z_q^{(1)}\right]=\begin{cases}\beta_1\dfrac{a_1^{\,2}\lambda_s}{3}+\lambda_n, & q=s;\\ \lambda_n, & q\neq s.\end{cases} \qquad (3)$$

where β_1 is a gain factor that follows from the fact that (S) might be closer to (R) than it is to (D). In other words, the received optical energy at (R) corresponding to E_s (that corresponds to the S-D link) is $\beta_1 E_s$. Performing a typical link budget analysis [4] shows that $\beta_1=\left(\dfrac{d_{SD}}{d_{SR}}\right)^2$ where d_{SD} and d_{SR} stand for the distances from (S) to (D) and (S) to (R) respectively.

The maximum-likelihood (ML) decision rule at (R) is given by: $\hat{s}=\arg\max_{q=1....Q} Z_q^{(1)}$. The relay transmits the symbol $\hat{s}$ along the link R-D implying that the corresponding decision vector can be written as $Z^{(2)}=\left[Z_1^{(2)},.....,Z_Q^{(2)}\right]$ where $Z_q^{(2)}$ is a Poisson r.v. with:

$$E\left[Z_q^{(2)}\right]=\begin{cases}\beta_2\dfrac{a_2^{\,2}\lambda_s}{3}+\lambda_n, & q=\hat{s};\\ \lambda_n, & q\neq\hat{s}.\end{cases} \qquad (4)$$

where $\beta_2=\left(\dfrac{d_{SD}}{d_{RD}}\right)^2$ with d_{RD} corresponding to the distance between (R) and (D).

Finally, note that the normalization of λ_s by 3 in equations (1), (3) and (4) ensures that the total transmit power is the same as in non-cooperative systems.

III. Receiver Structure

As in all cooperative schemes, decoding will be based on the assumption: $p_e \overset{\Delta}{=} P_r(\hat{s} \neq s) << 1$. This is justified since these schemes result in performance gains only for large values of E_s.

A. Detection in the Absence of Background Radiation

In the absence of background radiation, $Z^{(0)}$ and $Z^{(2)}$ contain at least $Q-1$ empty slots each. In this case, the detection procedure at (D) is as follows. If one component of $Z^{(0)}$ is different from zero, this will imply that the symbol s was transmitted in the corresponding slot since in the absence of background radiation the only source of this nonzero count is the presence of a light signal in this slot. On the other hand, if all components of $Z^{(0)}$ are equal to zero, then the decision will be based on $Z^{(2)}$. If one component of $Z^{(2)}$ is different from zero, then with probability $1-p_e$ this component corresponds to s and with probability p_e this component corresponds to an erroneous slot. Since $1-p_e$ is assumed to be greater than p_e (since $pe \ll 1$), then the best strategy is to decide in favor of the nonempty slot of $Z^{(2)}$. Finally, if all components of $Z^{(0)}$ and $Z^{(2)}$ are equal to zero, then (D) decides randomly in favor of one of the Q slots.

To summarize, (D) decides in favor of $\tilde{s}$ according to the following strategy:

$$\tilde{s} = \begin{cases} \arg_q\left[Z_q^{(0)} \neq 0\right], & Z^{(0)} \neq 0_Q ; \\ \arg_q\left[Z_q^{(2)} \neq 0\right], & Z^{(0)} = 0_Q, Z^{(2)} \neq 0_Q ; \\ rand(1,...,Q), & Z^{(0)} = Z^{(2)} = 0_Q . \end{cases} \tag{5}$$

where 0_Q corresponds to the Q-dimensional all-zero vector while the function $rand(1,...,Q)$ corresponds to choosing randomly one integer in the set $\{1, \ldots, Q\}$.

B. Detection in the Presence of Background Radiation

In this case, the background radiation results in nonzero counts even in empty slots necessitating a more complicated detection procedure.

The optimal ML detection procedure must take into consideration that $\hat{s}$ might be different from s. Note that $\hat{s} = s$ with probability $1 - p_e$ while $\hat{s}$ can correspond to a certain slot that is different from s with probability $\frac{p_e}{Q-1}$. In this case, eliminating all common terms in the log-likelihood function, it can be proven that the ML decision rule is given by:

$$(\tilde{s}, \hat{s}) = \arg \max_{q,q' \in \{1,\ldots,Q\}} \left[Z_q^{(0)} \ln\left(1 + \frac{a_0^2 \lambda_s}{3\lambda_n}\right) + Z_{q'}^{(2)} \ln\left(1 + \beta_2 \frac{a_2^2 \lambda_s}{3\lambda_n}\right) \right] + \begin{cases} \ln(1 - p_e), & q = q'; \\ \ln\left(\frac{p_e}{Q-1}\right), & q \neq q'. \end{cases} \quad (6)$$

Even though optimal, the above decoder is not feasible for practical implementation since it requires the knowledge of p_e which is not available. On the other hand, given that $p_e \ll 1$, then we can build a simpler decoder that is based on the assumption that the decision made at the relay is correct $(\hat{s} = s)$. In this case, the decision rule given in eq. (6) will simplify to:

$$\tilde{s} = \arg \max_{q \in \{1,\ldots,Q\}} \left[Z_q^{(0)} \ln\left(1 + \frac{a_0^2 \lambda_s}{3\lambda_n}\right) + Z_q^{(2)} \ln\left(1 + \beta_2 \frac{a_2^2 \lambda_s}{3\lambda_n}\right) \right] \quad (7)$$

Equation (7) corresponds to evaluating weighted sums of the photoelectron counts. An even simpler decision rule adopts equal weights and is given by:

$$\tilde{s} = \arg \max_{q \in \{1,\ldots,Q\}} \left[Z_q^{(0)} + Z_q^{(2)} \right] \qquad (8)$$

In this work, we adopt the equal-gain combiner (EGC) described in eq. (8) for the following reasons. First, simulations showed that the performance levels achieved by the decoders given in equations (6), (7) and (8) are very close to each other. In fact, for practical values of E_s, the decoders in equations (6) and (7) are extremely close to each other (which is justified since $p_e \ll 1$) and their performance gain with respect to EGC is negligible. Second, the implementation of EGC is much simpler since it does not require any form of training for acquiring the values of the channel gains as well as λ_s and λ_n.

Finally, equations (5) and (8) show that the proposed cooperation strategy can be implemented without requiring any channel state information neither at the transmitter nor at the receiver sides.

IV. Performance Analysis

Because of the symmetry of the PPM constellation, we evaluate the error performance of the proposed scheme assuming that the symbol s = 1 was transmitted.

A. No Background Radiation

The symbol-error probability (SEP) conditioned on the channel state $A \triangleq [a_0, a_1, a_2]$ is:

$$P_{e/A} = \Pr\left(Z_1^{(0)} > 0\right)p_0 + \Pr\left(Z_1^{(0)} = 0\right)\left[\Pr\left(Z_{\hat{s}}^{(2)} = 0\right)p_1 + \Pr\left(Z_{\hat{s}}^{(2)} > 0\right)\left((1-p_e)p_2 + p_e p_3\right)\right] \quad (9)$$

where $p_0 = 0$ since no error is made when there is at least one photoelectron in the first slot. $p_1 = \frac{Q-1}{Q}$ since when $Z^{(0)} = Z^{(2)} = 0_Q$ a random decision is made among the Q slots. $p_2 = 0$ since when a correct decision is made at (R) ($\hat{s} = 1$ with probability $1 - p_e$) and $Z_1^{(2)} > 0$, a correct decision will be made at (D) as well. Finally, $p_3 = 1$ since when (R) decides erroneously in favor of a symbol $\hat{s} \neq 1$ (with probability pe) and the count in the corresponding $\hat{s} - th$ slot of $Z^{(2)}$ is nonzero, then (D) will also decide in favor of $\hat{s}$ resulting in an error.

From eq. (3) the probability of error at (R) is $p_e = \frac{Q-1}{Q}\Pr\left(Z_1^{(1)} = 0\right) = \frac{Q-1}{Q}e^{-\beta_1 \frac{a_1^2 \lambda_s}{3}}$.

From eq. (1), $\Pr\left(Z_1^{(0)} = 0\right) = 1 - \Pr\left(Z_1^{(0)} > 0\right) = e^{-\frac{a_0^2 \lambda_s}{3}}$ and from eq. (4), $\Pr\left(Z_{\hat{s}}^{(2)} = 0\right) = 1 - \Pr\left(Z_{\hat{s}}^{(2)} > 0\right) = e^{-\beta_2 \frac{a_2^2 \lambda_s}{3}}$.

Replacing these probabilities as well as $p_0, \ldots\ldots, p_3$ in eq. (9) results in:

$$P_{e/A} = \frac{Q-1}{Q}\left[e^{-\left(a_0{}^2+\beta_2 a_2{}^2\right)\lambda_s/3} + e^{-\left(a_0{}^2+\beta_1 a_2{}^2\right)\lambda_s/3} - e^{-\left(a_0{}^2+\beta_2 a_2{}^2+\beta_2\ a_2{}^2\right)\lambda_s/3} \right] \qquad (10)$$

The SEP can be determined from:

$$P_e = \int_0^{+\infty}\int_0^{+\infty}\int_0^{+\infty} P_{e/A}\, f_A(a_0)\, f_A(a_1)\, f_A(a_2)\, da_0\, da_1\, da_2 \qquad (11)$$

where because of the form of $P_{e/A}$, the above integral can be split into three separate integrals.

For lognormal fading, eq. (11) does not admit a closed-form solution and it can be written as:

$$P_e = \frac{Q-1}{Q}\left[P_{e,0}P_{e,2} + P_{e,0}P_{e,1} - P_{e,0}P_{e,1}P_{e,2}\right] \qquad (12)$$

where $P_{e,0} \overset{\Delta}{=} Fr\left(\frac{\lambda_s}{3},0,\sigma\right)$, $P_{e,1} \overset{\Delta}{=} Fr\left(\beta_1\frac{\lambda_s}{3},0,\sigma\right)$ and $P_{e,2} \overset{\Delta}{=} Fr\left(\beta_2\frac{\lambda_s}{3},0,\sigma\right)$ where $Fr(a,0,b)$ is the lognormal density frustration function defined in [11] as:

$$Fr(a,0,b) = \int_0^{+\infty} \frac{1}{\sqrt{2\pi b^2}\,x}\exp\left(-ax^2\right)\exp\left[-\frac{\left(\ln(x)+b^2\right)^2}{2b^2}\right]dx \qquad (13)$$

Equation (12) shows that P_e is large when either the links S-D and R-D are both in deep fades or when the links S-D and S-R are both in deep fades thus reflecting the enhanced diversity order of the proposed cooperative system. In the case of Rayleigh fading, the integrals in eq. (11) can be readily solved resulting in:

$$P_e = \frac{Q-1}{Q}\left[\frac{1}{\left(1+\frac{\lambda_s}{3}\right)\left(1+\beta_2\frac{\lambda_s}{3}\right)} + \frac{1}{\left(1+\frac{\lambda_s}{3}\right)\left(1+\beta_1\frac{\lambda_s}{3}\right)} - \frac{1}{\left(1+\frac{\lambda_s}{3}\right)\left(1+\beta_1\frac{\lambda_s}{3}\right)\left(1+\beta_2\frac{\lambda_s}{3}\right)}\right] \qquad (14)$$

The last equation (14) shows that P_e scales asymptotically as λ_s^{-2} (rather than λ_s^{-1} as in 1×1 non-cooperative FSO links) showing that the diversity order of the proposed scheme is two.

B. With Background Radiation

In the presence of background radiation, the conditional probability of error is given by:

$$P_{e/A} = (1 - p_e)P_{e/A,\hat{s}=1} + p_e P_{e/A,\hat{s}\neq 1} \qquad (15)$$

Define the vector Z as: $Z = \lfloor Z_{1,}.....,Z_Q \rfloor = Z^{(0)} + Z^{(2)}$. When $\hat{s} = 1$, the parameter of the Poisson r.v. Z_1 is: $\left\lfloor \left(a_0{}^2 \lambda_s/3 + \lambda_n\right) + \left(\beta_2 a_2{}^2 \lambda_s/3 + \lambda_n\right) \right\rfloor = \left\lfloor \left(a_0{}^2 + \beta_2 a_2{}^2\right)\lambda_s/3 + 2\lambda_n \right\rfloor$ while Z_2,.....Z_Q are Poisson r.v.s with parameters $2\lambda_n$. Ignoring the probability of correct decision when ties occur, $P_{e/A,\hat{s}} = 1$ can be upper-bounded by:

$$P_{e/A,\hat{s}=1} = 1 - P_{c/A,\hat{s}=1} \le 1 - \Pr(Z_2 < Z_1)...\Pr(Z_Q < Z_1) = 1 - \left[\Pr(Z_2 < Z_1)\right]^{Q-1}$$

$$= 1 - \left[\sum_{k=0}^{+\infty} \frac{e^{-\left(\left(a_0{}^2 + \beta_2 a_2{}^2\right)\lambda_s/3 + 2\lambda_n\right)}\left(\left(a_0{}^2 + \beta_2 a_2{}^2\right)\lambda_s/3 + 2\lambda_n\right)^k}{k!} \sum_{j=0}^{k-1} \frac{e^{-2\lambda_n}(2\lambda_n)^j}{j!}\right]^{Q-1} \qquad (16)$$

On the other hand, when $\hat{s} \neq 1$, Z_1 has a parameter of $\left(a_0{}^2 \lambda_s/3 + 2\lambda_n\right)$, $Z_{\hat{s}}$ has a parameter of $\left(\beta_2 a_2{}^2 \lambda_s/3 + 2\lambda_n\right)$ while the parameters of the remaining components are all equal to $2\lambda_n$. Consequently, $P_{e/A,\hat{s}\neq 1}$ can be upper-bounded by:

$$P_{e/A,\hat{s}\neq 1} \le 1-\Pr(Z_2 < Z_1)...\Pr(Z_Q < Z_1) = 1-\left[\Pr\left(Z_q < Z_1\right)\right]^{Q-1}\Pr\left(Z_{\hat{s}} < Z_1\right); \quad q \neq 1,\hat{s}$$

$$= 1-\left[\sum_{k=0}^{+\infty}\frac{e^{-\left(a_0{}^2\lambda_s/3+2\lambda_n\right)}\left(a_0{}^2\lambda_s/3+2\lambda_n\right)^k}{k!}\sum_{j=0}^{k-1}\frac{e^{-2\lambda_n}\left(2\lambda_n\right)^j}{j!}\right]^{Q-2} \times$$

$$\left[\sum_{k=0}^{+\infty}\frac{e^{-\left(a_0{}^2\lambda_s/3+2\lambda_n\right)}\left(a_0{}^2\lambda_s/3+2\lambda_n\right)^k}{k!}\sum_{j=0}^{k-1}\frac{e^{-\left(\beta_2 a_2{}^2\lambda_s/3+2\lambda_n\right)}\left(\beta_2 a_2{}^2\lambda_s/3+2\lambda_n\right)^j}{j!}\right] \quad (17)$$

Finally, based on a similar approach, p_e in eq. (15) can be upper-bounded by:

$$p_e \le 1-\left[\sum_{k=0}^{+\infty}\frac{e^{-\left(\beta_1 a_1{}^2\lambda_s/3+\lambda_n\right)}\left(\beta_1 a_1{}^2\lambda_s/3+\lambda_n\right)^k}{k!}\sum_{j=0}^{k-1}\frac{e^{-\lambda_n}\lambda_n{}^j}{j!}\right]^{Q-1} \quad (18)$$

Because of the complexity of the terms in equations (16)-(18), eq. (15) does not lend itself to a simple mathematical evaluation and p_e does not admit a closed-form solution in both lognormal and Rayleigh fading. In this case, the integrals in eq. (11) must be evaluated numerically.

V. Numerical Results

In this section, we present numerical results for the error performance of FSO links with and without cooperation. In what follows, we assume that $d_{SD} = d_{RD}$ implying that $\beta_2 = 1$. The performance of the 2 × 1 MIMO-FSO links in [4] that deploy repetition coding (RC) and that are capable of achieving a full transmit diversity order is also included as a benchmark.

Fig. 9 shows the performance of 4-PPM in the absence of background radiation over Rayleigh fading channels.

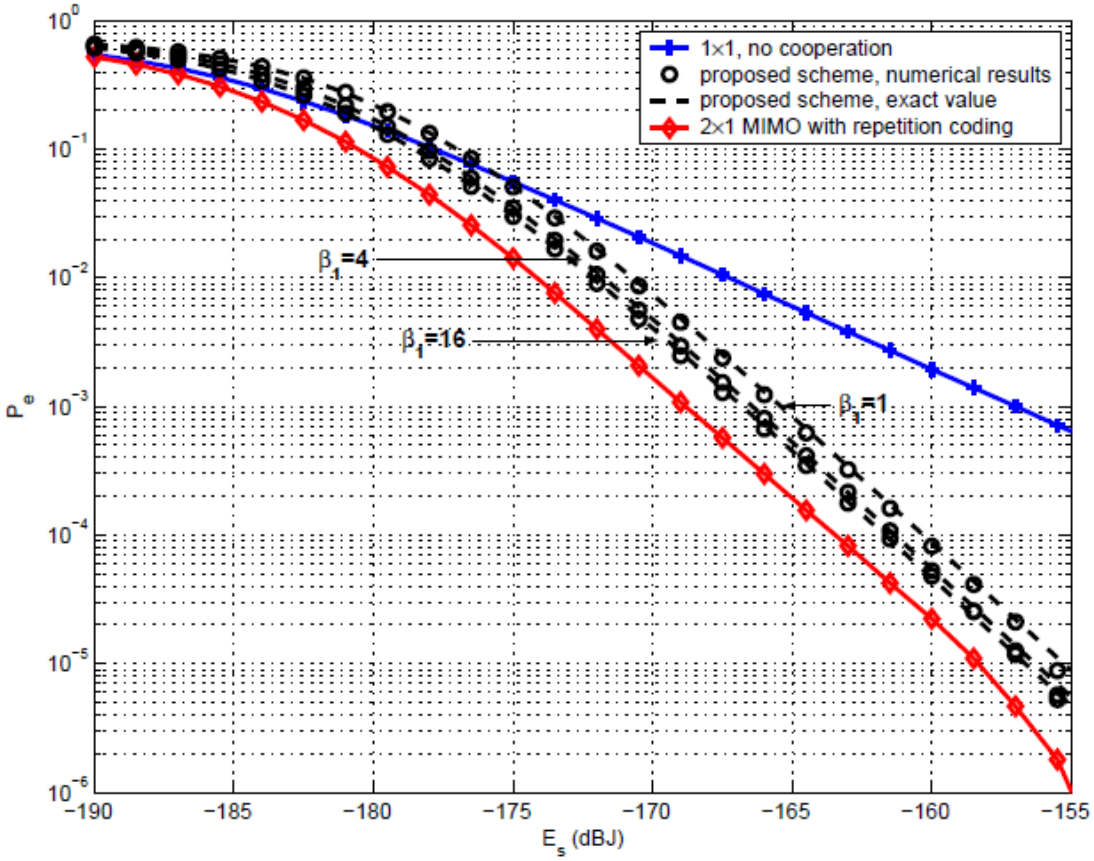

Figure 9: Performance of 4-PPM for the Rayleigh fading case with no background radiation. This figure also shows the performance of the 2 × 1 MIMO diversity scheme proposed in [4].

This figure shows the excellent match between simulations and the exact SEP expression in eq. (14). The slopes of the SEP curves indicate that cooperation results in an increased

diversity order of two for various distances of (R) from (S). Even in the extreme case where (S) is as far from (R) as it is from (D) ($\beta_1 = 1$), a gain of about 8 dB at a SEP of 10^{-3} can be observed relative to non-cooperative systems. The excellent match between simulations and eq. (12) can be seen in Fig. 10 where a similar simulation setup is adopted in the case of lognormal fading with S.I. = 0.6.

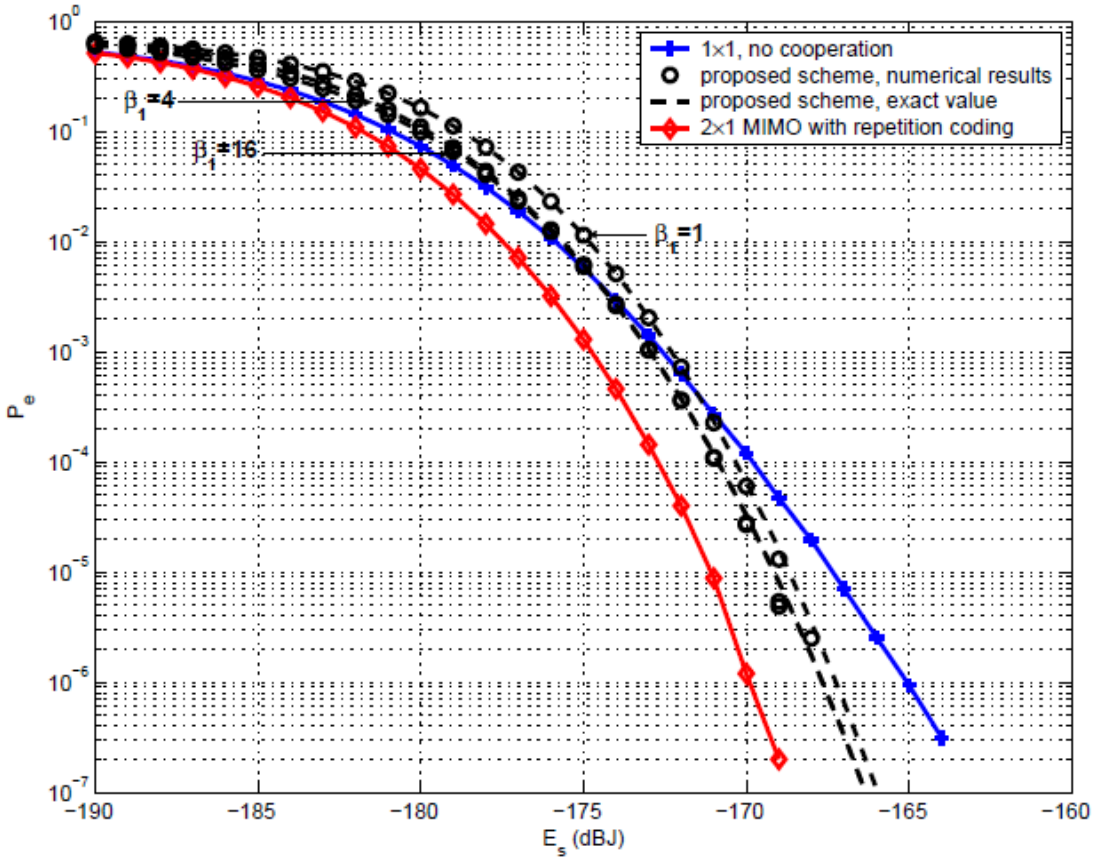

Figure 10: Performance of 4-PPM for the lognormal fading case (S.I. = 0.6) with no background radiation. This figure also shows the performance of the 2 × 1 MIMO diversity scheme proposed in [4].

Results in Fig. 9 and Fig. 10 show that cooperation is more beneficial in the case of Rayleigh fading compared to lognormal fading where the performance gain can be realized at smaller error rates. This result is expected since the Rayleigh distribution is used to model the scenario of severe fading while the lognormal model corresponds to the scenario of less severe fading. The superiority of the cooperative scheme over non-

cooperative direct FSO links can be also seen in Fig. 11 in the presence of background radiation.

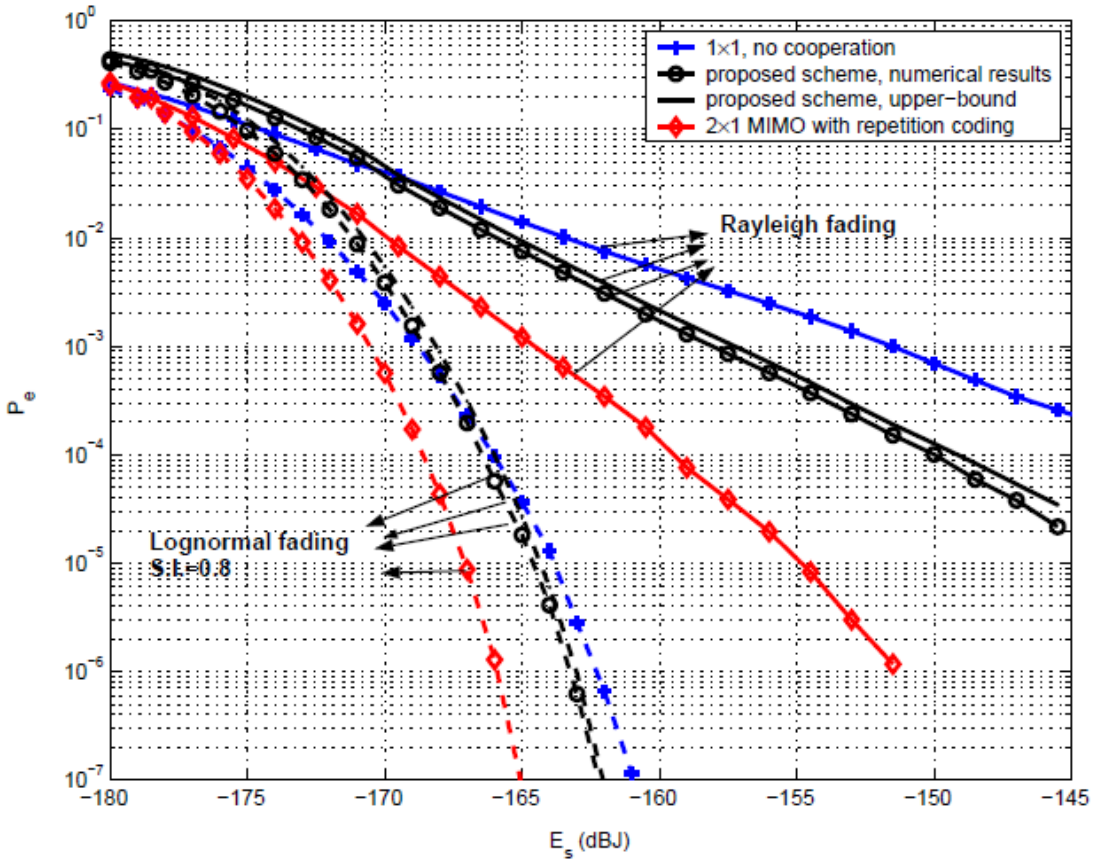

Figure 11: Performance of 4-PPM in the presence of background radiation with $P_b T_s / Q = -185\ dBJ$. For the cooperative scheme, β_1 = 4 and β_2 = 1. The upper-bounds are obtained from the numerical integration of the conditional probability of error given in eq. (15)-(18). This figure also shows the performance of the 2 × 1 MIMO diversity scheme proposed in [4].

As in the no-background radiation case, gains are more significant over Rayleigh fading channels.

While the assumption of channel independence can be justified in MIMO wireless RF systems, there is a wide agreement that this assumption is not often valid in MIMO-FSO systems and, consequently, the high gains promised by MIMO techniques might not be realized in practice. This point is investigated in Fig. 12 that compares the proposed cooperative system with the 2×1 MIMO-RC system in the presence of channel correlation.

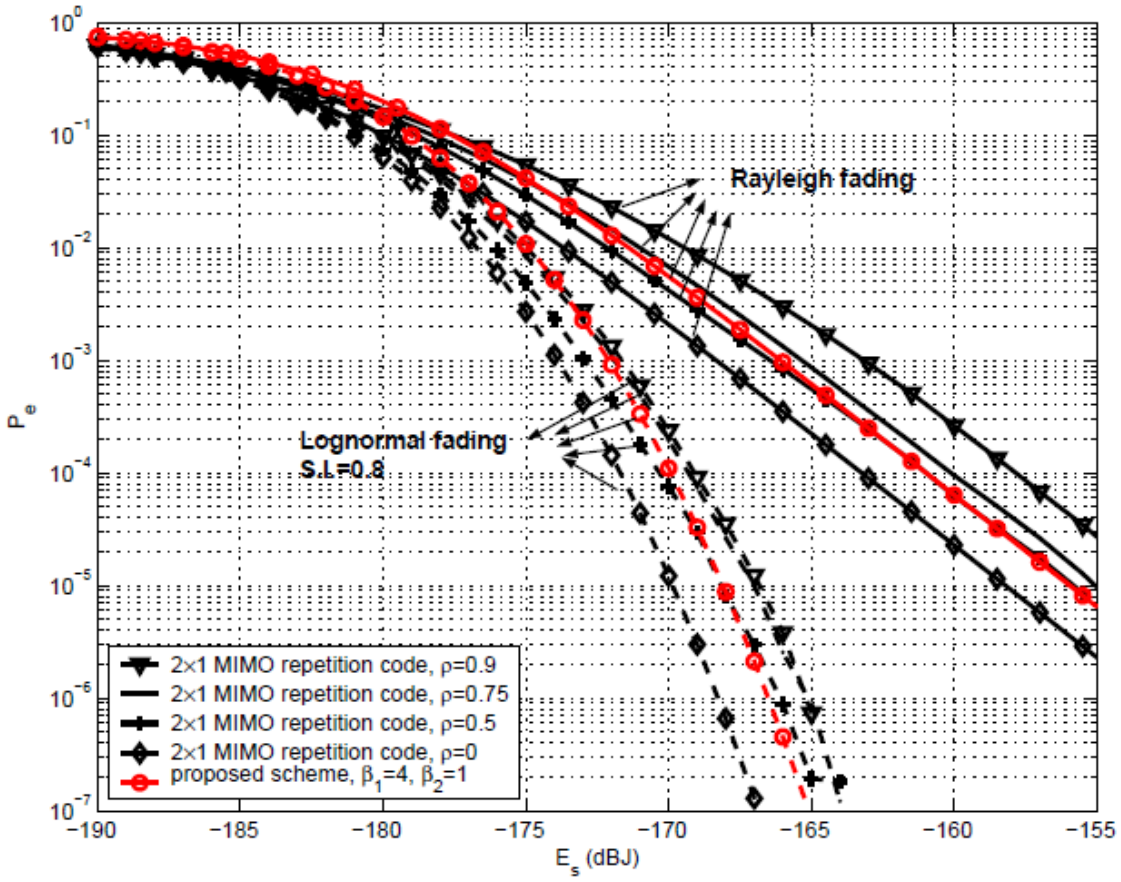

Figure 12: Performance of 8-PPM in the absence of background radiation. The parameter ρ corresponds to the correlation between the two 2 × 1 MIMO co-channels. For the MIMO systems, the repetition code proposed in [4] is employed.

Results show that, for relatively large values of E_s, the cooperative scheme shows approximately the same performance as the MIMO-RC system with a channel correlation factor of $\rho = 0.5$. The proposed scheme can even outperform MIMO-RC systems when $\rho = 0.75$ or $\rho = 0.9$.

VI. Future Work

The performance analysis and the numerical values illustrated in this work regarding the proposed cooperative diversity technique were done based on the fact that the transmitted power from transceivers $TRx_{S,1}$, $TRx_{S,2}$ and $TRx_{R,2}$ are to be divided by 3. However, this approach doesn't necessarily guarantee the realization of the optimal solution concerning symbol-error probability (SEP). Taking this into consideration, it would be essential to consider some analytic mathematical approaches that would present a solution for the optimal ratio values for the power transmitted from $TRx_{S,1}$, $TRx_{S,2}$ and $TRx_{R,2}$ and thus the optimal value for SEP. In other words, instead of distributing the power equally among the transceivers (S), (R) & (D) as it is the case in our study, it might be optimal if transceivers (S), (R) & (D) transmit $P_r/2$, $P_r/4$, $P_r/4$ respectively for a given channel state. Certainly, this approach would impose the installation of a more sophisticated receiver but the enhancement in the performance would compensate for this cost penalty.

Karush-Kuhn-Tucker (KKT) theorem, used for a solution in nonlinear programming, is one of the analytical approaches that would be extensively studied in any future work. Notwithstanding, this theorem was implemented in MatLab using non-linear function as it is shown in Appendix B -for the case of Rayleigh fading and no background radiation- to get a sort of sense concerning the optimal power ratio results that might be different from those assumed in our study (equally distributed).

Let the power transmitted from $TRx_{S,1}$, $TRx_{S,2}$ and $TRx_{R,2}$ be distributed as following $t0.P_r$, $t1.P_r$, $t2.P_r$ respectively, where $t0$, $t1$, $and\, t2$ are real values satisfying the following constrains: 1- $t0 + t1 + t2 = 1$

2- $t0 \geq 0;\ t1 \geq 0;\ t2 \geq 0$

Table 1, 2 & 3 illustrates the optimal values for $t0$, $t1$, $and\, t2$ simulated over 28 channel state $A \overset{\Delta}{=} [a_0, a_1, a_2]$ at E_s =-160 dBJ, -170 dBJ & -190 dBJ respectively using the KKT theorem.

t0	t1	t3
1	2.22E-16	2.22E-16
1	2.22E-16	2.22E-16
1	0	0
1	1.67E-16	1.67E-16
0.5	0.25	0.25
1	1.67E-16	1.67E-16
1	5E-16	8.91E-28
1	7E-27	5E-16
1	1.67E-16	1.67E-16
1	6.01E-28	4.44E-16
1	2.78E-16	2.78E-16
1	1.67E-16	1.67E-16
1	1.67E-16	1.67E-16
1	0	0
1	1.67E-16	1.67E-16
1	5.66E-27	3.89E-16
1	1.86E-27	4.44E-16
1	4.44E-16	2.13E-27
1	2.94E-27	3.89E-16
1	1.64E-27	3.89E-16
1	0	0
1	1.67E-16	1.67E-16
1	1.67E-16	1.67E-16
1	3.89E-16	3.96E-28
1	2.22E-16	2.22E-16
1	0	0
1	2.22E-16	2.22E-16

Table 1: Optimal power ratios t0, t1, t2 simulated over 28 channel state $\overset{\Delta}{A}=[a_0,a_1,a_2]$ at Es=-160 dBJ using KKT.

t0	t1	t2
1	0	1.11E-16
1	2.78E-16	2.78E-16
1	0	0
1	-1.1E-16	0
0.423895	0	0.576105
1	0	-1.1E-16
1	0	0
0.5	0.250006	0.249994
0.500125	0.250237	0.249638
0.5	0.246787	0.253213
0.497641	0.225361	0.276998
1	1.99E-32	0
0.500067	0.499933	1.39E-17
1	0	0
0.995596	5.47E-08	0.004404
1	0	-1.1E-16
0.477106	0.081233	0.441661
0.999986	-1.1E-16	1.41E-05
0.5	0.5	-1.1E-16
1	1.09E-26	5E-16
0.49851	0.18467	0.31682
1	0	2.51E-25
1	2.22E-16	2.22E-16
1	2.22E-16	2.22E-16
1	0	0
1	5.55E-16	0
1	0	1.11E-16

Table 2 : Optimal power ratios t0, t1, t2 simulated over 28 channel state $A \overset{\Delta}{=} [a_0, a_1, a_2]$ at Es=-170 dBJ using KKT.

t0	t1	t2
0.750306	0.249693	4.84E-07
0.803941	3.41E-10	0.196059
0.538608	0	0.461392
0.946942	0.013937	0.039121
0.583903	0.328731	0.087366
1	5.55E-17	0
0.829768	0.035128	0.135104
0.402762	0.597238	7.45E-10
2.61E-23	1	3.33E-07
1.23E-07	1	0
0.906305	8.96E-16	0.093695
0.038031	0.549969	0.412
-1.8E-24	1	1.49E-08
7.69E-19	0.335932	0.664068
0.078987	0.103531	0.817481
1.26E-07	1	0
1.27E-08	1	0
0.994311	0.005689	0
2.11E-28	0.173654	0.826346
0.462868	0.241344	0.295787
0.989183	4.93E-32	0.010817
3.78E-08	1	0
6.63E-23	5.36E-07	0.999999
1	0	2.46E-32
1	1.23E-32	2.78E-17
3.43E-07	1	0
0.750306	0.249693	4.84E-07

Table 3: Optimal power ratios t0, t1, t2 simulated over 28 channel state $A \overset{\Delta}{=} [a_0, a_1, a_2]$ at Es=-190dBJ using KKT.

These tables illustrate the fact that distributing the power equally among the transceivers $TRx_{S,1}$, $TRx_{S,2}$ and $TRx_{R,2}$ doesn't necessarily achieve the optimal value of SER. This result is expected for the reason that the path gains (a0, a1, a2) of our channel model varies. Thus eq. (10), eq. (16) & eq. (18) would be extensively expressed as follows respectively:

$$P_{e/A} = \frac{Q-1}{Q}\left[e^{-\left(a_0{}^2.t0+\beta_2 a_2{}^2.t2\right)\lambda_s} + e^{-\left(a_0{}^2.t0+\beta_1 a_2{}^2.t1\right)\lambda_s} - e^{-\left(a_0{}^2.t0+\beta_2 a_2{}^2.t1+\beta_2\ a_2{}^2.t2\right)\lambda_s} \right] \tag{10.1}$$

$$P_{e/A.\hat{s}=1} = 1-\left[\sum_{k=0}^{+\infty} \frac{e^{-\left(\left(a_0{}^2.t0+\beta_2 a_2{}^2.t2\right)\lambda_s+2\lambda_n\right)}\left(\left(a_0{}^2.t0+\beta_2 a_2{}^2.t2\right)\lambda_s+2\lambda_n\right)^k}{k!} \sum_{j=0}^{k-1} \frac{e^{-2\lambda_n}(2\lambda_n)^j}{j!} \right]^{Q-1} \tag{16.1}$$

$$p_e \le 1-\left[\sum_{k=0}^{+\infty} \frac{e^{-\left(\beta_1 a_1{}^2.t1.\lambda_s+\lambda_n\right)}\left(\beta_1 a_1{}^2.t1.\lambda_s+\lambda_n\right)^k}{k!} \sum_{j=0}^{k-1} \frac{e^{-\lambda_n}\lambda_n{}^j}{j!} \right]^{Q-1} \tag{18.1}$$

In other words knowing the channel path gain values a0, a1 and a2, KKT theorem would be directly applied to obtain the optimal values: $t0,\ t1,\ and\ t2$.

However and in the context of optimal values' investigation, a sub-optimal algorithm could be presented instead of that distributing the power equally among the transceivers and thus offering better values for $t0,\ t1,\ and\ t2$ which in returns enhance the SEP.

The proposed algorithm works as following:

1- Calculate the SEP for our proposed cooperative technique at a given channel state $A \overset{\Delta}{=} [a_0, a_1, a_2]$ for $t0,\ t1,\ and\ t2$ equal to 1, 0, and 0 respectively.

2- Calculate the SEP for our proposed cooperative technique at the same given channel state $A \overset{\Delta}{=} [a_0, a_1, a_2]$ for $t0 = 0$, $t1\ and\ t2$ to be calculated such that SEP is minimum.

3- Finally, compare the values of SEP in step1 and step 2 and choose the values of $t0,\ t1,\ and\ t2$ that result in minimal SEP.

Fig. Illustrates the enhancement offered by the proposed algorithm. For example, for $P_e = 10^{-3}$ an improvement of 6 dBJ is noticed.

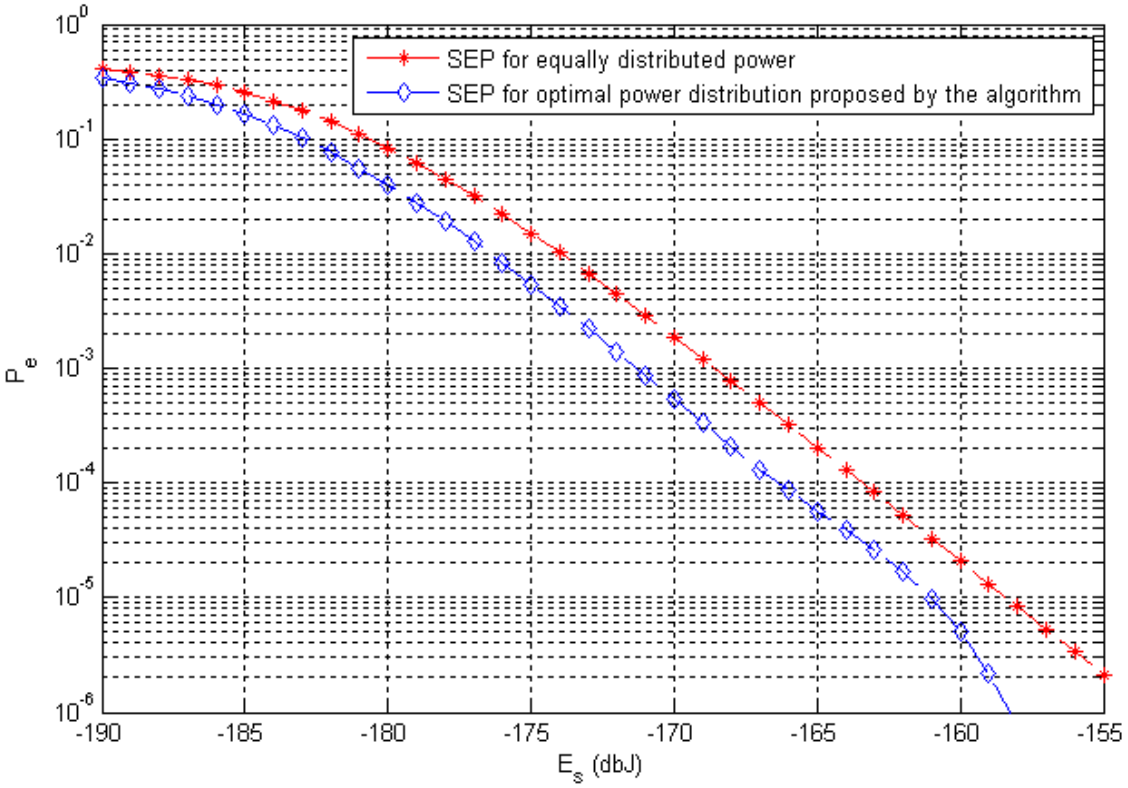

Figure 13: Enhancement in SEP offered by the proposed algorithm.

On the other hand and in this context also, SISO and 2x1 MIMO could be implemented as forms of special cases for our proposed technique. This is also done but this time by selecting the values of $t0$, $t1$, $and\, t2$ rather than applying mathematical theorem:

a- SPECIAL CASE 1: NO BACKGROUND RADIATION

1- Single Input Single Output (SISO): This system (SISO) can be implemented using our proposed cooperative technique by simply isolating the relay transceiver (R). In other words, instead of distributing the transmitted power P_r among the transceivers (S), (R) & (D), simply we allocate all the power transmitted P_r on the channel linking transceivers (S) & (D) only.

Mathematically this could be represented by substituting $t0,\ t1,\ and\ t2$ in eq. (10.1) by the values 1, 0, and 0 respectively. Replacing these values in eq. (10.1) results in :

$$P_{e/A} = \frac{Q-1}{Q}\left[e^{-\left(a_0{}^2\right)\lambda_s}\right]$$

which is the case of SISO systems as listed in eq. (13) in [4].

2- Multiple Inputs Multiple Outputs (MIMO): The proposed cooperative diversity technique could be also deployed as a 2x1 MIMO system. To achieve this step, three issues are to be considered:

a- The gain factor β_2 is set up to be 1 assuming that $d_{SD} = d_{SR}$

b- The power transmitted between (S) and (R) is assumed infinite ($t1 = \infty$)

c- Power transmitted from (S) & (R) to (D) is equally distributed. In other words, the values of $t0,\ and\ t2$ are 0.5 & 0.5 respectively.

Taking these issues into consideration and replacing $t0,\ t1,\ and\ t2$ in eq. (10.1) & eq. (11) results in:

$$P_e = \int_0^{+\infty}\int_0^{+\infty} P_{e/A}\, f_A(a_0)\, f(a_2)\, da_0\, da_2$$

where $P_{e/A} = \frac{Q-1}{Q}\left[e^{-\left(a_0{}^2.(0.5)+\beta_2 a_2{}^2.(0.5)\right)\lambda_s}\right]$

This would confirm eq. (17) in [4] for the case of 2x1 MIMO transmissions in case of fading & no background radiation.

b- SPECIAL CASE 2: WITH BACKGROUND RADIATION

1- Single Input Single Output (SISO): Holding the same procedures as mentioned in **SPECIAL CASE 1** and replacing the same values of $t0,\ t1,\ and\ t2$ in eq. (15), eq. (16.1) and eq. (18.1) results in:

a- $p_e = 0$

b- $P_{e/A} = P_{e/A,\hat{s}=1}$

c- Noise being produced in the presence of one receiver only and thus it is equal to λ_n rather than $2\lambda_n$

As a result, the probability of error is:

$$P_{e/A} = 1 - \left[\sum_{k=0}^{+\infty} \frac{e^{-\left(\left(a_0{}^2\right)\lambda_s + \lambda_n\right)} \left(\left(a_0{}^2\right)\lambda_s + \lambda_n\right)^k}{k!} \sum_{j=0}^{k-1} \frac{e^{-\lambda_n} \left(\lambda_n\right)^j}{j!} \right]^{Q-1}$$

which confirm the result presented in eq. (22) in [4] for the case of SISO.

2- Multiple Inputs Multiple Outputs (MIMO): As in **SPECIAL CASE 1,** β_2 is set up to be equal to 1, power transmitted from (S) to (R) is assumed infinite ($t1 = \infty$), and the values of $t0,\ and\ t2$ are 0.5 & 0.5 respectively. Replacing these values in eq. (15), eq. (16.1) and eq. (18.1) results in:

a- $p_e = 0$

b- $P_{e/A} = P_{e/A,\hat{s}=1}$

c- Noise being produced in the presence of one receiver only and thus it is equal to λ_n rather than $2\lambda_n$

As a result, the probability of error in the presence of background noise radiation is:

$$P_{e/A} = P_{e/A,\hat{s}=1} = 1 - \left[\sum_{k=0}^{+\infty} \frac{e^{-\left(\left(a_0{}^2.(0.5)+a_2{}^2.(0.5)\right)\lambda_s+\lambda_n\right)} \left(\left(a_0{}^2.(0.5)+a_2{}^2.(0.5)\right)\lambda_s+\lambda_n\right)^k}{k!} \sum_{j=0}^{k-1} \frac{e^{-\lambda_n}(\lambda_n)^j}{j!} \right]^{Q-1}$$

which confirms eq. (22) in [4] for the case of 2x1 MIMO.

On the other hand and in the context of future work, it is undoubted that the Radio Frequency (RF) spectrum will not be enough to support additional capacity in the future meantime taking into consideration, particularly, the huge data exchanged between earth and space (satellites). This will certainly open the door extensively towards the free space optical communications as a vital solution for '*creating a three-dimensional global communications grid of inter-connected ground & airborne nodes*'. Hence the unlimited bandwidth provided by FSO communications will offer an essential subject on the table of research and thus make it worth to study our cooperative diversity technique in a network structure in any future work.

VII. Conclusion

Despite the non-broadcast nature of FSO transmissions, this work showed that cooperative diversity can result in significant performance gains over the non-cooperative 1×1 FSO links and over the 2×1 MIMO-FSO links that suffer from correlated fading. It was proven analytically that a full transmit diversity order of two can be achieved in the no-background radiation case. In the presence of background radiation, a numerical integration of the conditional SEP showed that the proposed scheme can maintain acceptable performance gains especially in the case of Rayleigh fading. While this work analyzed cooperative diversity from a physical-layer point of view, future work must consider the implication of cooperation on higher layers.

References

Kednar, D. & Arnon, S. (2003, February). Urban optical wireless communications networks: The main challenges and possible solutions. *IEEE Communications Magazine, 42*(5), 2-7.

Zhu, X. & Kahn, J. (2002, August). Free-space optical communication through atmospheric turbulence channels. *IEEE Transactions on Communications, 50*(8), 1293-1300.

Khalighi, M.G., Schwartz, N., Aitamer, N., & Bourennane, S. (2009, November). Fading reduction by aperture averaging and spatial diversity in optical wireless systems. *IEEE Journal of Optical Communications and Networking, 1*, 580-593.

Wilson, S. G., Brandt-Pearce, M., Cao, Q., & Leveque, J. H. (2005, August). Free-space optical MIMO transmission with Q-ary PPM. *IEEE Transactions on Communications, 53,* 1402-1412.

Simon, M. K., & Vilnrotter, V. A. (2005, January). Alamouti-type space-time coding for free-space optical communication with direct detection. *IEEE Transactions on Wireless Communications, 4,* 35-39.

Garcia-Zambrana, A., Castillo-Vazquez, C., Castillo-Vazquez, B., & Hiniesta-Gomez, A. (2009, July). Selection transmit diversity for FSO links over strong atmospheric turbulence channels. *IEEE Photonics Technology Letters, 21,* 1017-1019.

Navidpour, S., Uysal, M., & Kayehrad, M. (2007, August). BER performance of free-space optical transmission with spatial diversity. *IEEE Transactions on Wireless Communications, 6*(8), 2813-2819.

Tsiftsis, T., Sandalidis, H., Karagiannidis, G., & Uysal, M. (2009, February). Optical wireless links with spatial diversity over strong atmospheric turbulence channels. *IEEE Transactions on Wireless Communications, 8*(2), 951-957.

Laneman, J. & Wornell, G. (2003, October). Distributed space time coded protocols for exploiting cooperative diversity in wireless networks. *IEEE Transactions on Information Theory,* 49(10), 2415-2425.

Laneman, J., Tse, D., & Wornell G. (2004, December). Cooperative diversity in wireless networks: Efficient protocols and outage behavior. *IEEE Transactions on Information Theory, 50,* 3062-3080.

Halme, S., Levitt, B., & Orr, R. (1969). Bounds and approximations for some integral expression involving lognormal statistics. *MIT Research Lab for Electronics Quart Program Report.*

APPENDIX A:

MatLab code for the proposed cooperative technique in the absence of background radiation:

```
function
[errors_average_fading,prob_of_error]=symbole_Error_probability2(symbol
e_number,fading,Es,En,Q,SD,SR,RD)

% symbole_number is the number of symbols sent from the transceivers
% fading is a real value that specifies the model of fading whether
  Rayleigh or Log-normal. If the range is between 0.4 and 1 then it is
  Log-normal fading; if fading = 2 then there is no fading; if fading =
3
  then it is Rayleigh fading
% Es is the received optical energy per symbol
% En is the noise energy
% Q is the number of slots per symbol
% SD is the distance separating the source (S) and the destination (D)
% SR is the distance separating the source (S) and the relay (R)
% RD is the distance separating the relay (R) and the destination (D)



symbole1=floor(Q*rand(1,symbole_number))+1; %Generate a symbol vector
of length 'symbole_number'
for j=1:1:length(Es)
    symbole(:,:,j)=symbole1;
end

n=length(Es);
Ns1=(1/3)*0.5*(1/(6.625*10^-34*1.93*10^14))*10.^(Es/10); % number of
photoelectrons transmitted from (S) t0 (D)
Es2=Es+10*log10(SD^2/SR^2);
Ns2=(1/3)*0.5*(1/(6.625*10^-34*1.93*10^14))*10.^(Es2/10); % number of
photoelectrons transmitted from (S) t0 (R)
Es3=Es+10*log10(SD^2/RD^2);
```

```
Ns3=(1/3)*0.5*(1/(6.625*10^-34*1.93*10^14))*10.^(Es3/10); % number of
photoelectrons transmitted from (R) t0 (D)
Nb=0.5*(1/(6.625*10^-34*1.93*10^14))*(10^(En/10));% number of
photoelectrons generated in the presence of noise which is zero in our
case
errors_average_poission=zeros(1,n);

for fading_loop=1:1:4000 % Generate 4000 channel model of Rayleigh or
Log-normal fading

    s1=symbole_detection(symbole,fading,Ns1,Nb,Q); % s1 is the
symbole vector subjected to fading transmitted from (S) to (D)
    s2=symbole_detection1(symbole,fading,Ns2,Nb,Q); % s2 is the
symbole vector subjected to fading transmitted from (S) to (R)
    s3=symbole_detection(s2,fading,Ns3,Nb,Q);% s3 is the symbole
vector subjected to fading transmitted from (R) to (D)

errors_sum=zeros(1,length(Es));
count1=poissrnd(s1); % s1 modeled as a Poisson random variable (r.v.)
count3=poissrnd(s3); % s3 modeled as a Poisson random variable (r.v.)
[max_num1,Index1]=max(count1);
[max_num3,Index3]=max(count3);

% Receiver structure at (D): Detection in the Absence of Background
Radiation
for ii=1:1:length(Es)
    if length(find(max_num1(:,:,ii)))==symbole_number
        s_detected(:,:,ii)=Index1(:,:,ii);
    else
        Index_zero=find(max_num1(:,:,ii)==0);
        count1(:,Index_zero,ii)=count3(:,Index_zero,ii);
        [max_num4,Index4]=max(count1(:,:,ii));
        if length(find(max_num4))==symbole_number
            s_detected(:,:,ii)=Index4;
        else
          Index_zero2=find(max_num4==0);
```

```
count1(:,Index_zero2,ii)=(floor(Q*rand(length(Index_zero2),Q))+1)';
          [max_num5,Index5]=max(count1(:,:,ii));
          s_detected(:,:,ii)=Index5;
        end
    end
end
s=symbole- s_detected;

% error detection
for j=1:1:length(Es)
errors_sum(j)=errors_sum(j)+length(nonzeros(s(:,:,j)));
end
for jj=1:1:length(Es)
errors_average_poission(1,jj)=errors_average_poission(1,jj)+errors_sum(
jj)/1;%average number of error
end
end
errors_average_fading=errors_average_poission/4000;
prob_of_error=errors_average_fading/symbole_number;% probability of
error
semilogy(Es,prob_of_error,'b--'),grid;
xlabel('E_s in db');
ylabel('P_s');
axis([Es(1,1),Es(1,n),10^-12,1]);
```

```
function symbole_detected=symbole_detection(symbole,fading,Ns,Nb,Q)


if fading<=1
varience=0.25*log(fading+1);
mean=-1*varience;
end
 a_gain=1; % path gain between the transceivers due to fading
   if fading<=1
         a_gain=lognrnd(mean,sqrt(varience));
    elseif fading==2
            a_gain=1;
    elseif fading==3
         a_gain=raylrnd(1/sqrt(2));
   end
   I=eye(Q);

for i=1:1:length(Ns)
    parameter=a_gain^2*Ns(i)*I(:,symbole(:,:,i))+Nb;
    C(:,:,i)=parameter;
end
symbole_detected=C;
```

```
function symbole_detected=symbole_detection1(symbole,fading,Ns,Nb,Q)


if fading<=1
varience=0.25*log(fading+1);
mean=-1*varience;
end
 a_gain=1; % path gain between the transceivers due to fading
   if fading<=1
         a_gain=lognrnd(mean,sqrt(varience));
    elseif fading==2
            a_gain=1;
    elseif fading==3
         a_gain=raylrnd(1/sqrt(2));
   end
   I=eye(Q);
for i=1:1:length(Ns)
    parameter=a_gain^2*Ns(i)*I(:,symbole(:,:,1))+Nb;
    C(:,:,i)=parameter;
end
% % Receiver structure at (R): Detection in the Absence of Background
Radiation
count=poissrnd(C);
[max_num,Index]=max(count);
if length(find(max_num))==length(symbole)
   symbole_detected=Index;
else
   Index_zero=find(max_num==0);
   count(:,Index_zero)=(floor(Q*rand(length(Index_zero),Q))+1)';
   [max_num1,Index1]=max(count);
   symbole_detected=Index1;
end
```

APPENDIX B:

MatLab code for the Karush-Kuhn-Tucker theorem applied to our proposed cooperative technique in the absence of background radiation:

```
function [P0,P1,P2,fval1]= Min_Prob

A=[1 0 0;0 1 0;0 0 1];
b=[1;1;1];
Aeq=[1 1 1];
beq=[1];
lb=[0;0;0];
ub=[1;1;1];
fval=0;

for i=1:1:500 % Generate 500 channel model of Rayleigh or Log-normal
fading
    [P,fval]=fmincon(@myfun,[0 0 0],A,b,Aeq,beq,lb,ub); % Karush-Kuhn-
Tucker (KKT)

    P0(i)=P(1);
    P1(i)=P(2);
    P2(i)=P(3);

    fval=fval+fval;
end
fval1=fval/500;
```

```
function f = myfun(P)

Ns=0.5*(1/(6.625*10^-34*1.93*10^14))*10^(-170/10); % number of
photoelectrons transmitted with optical energy of -170 dBJ

a0=raylrnd(1/sqrt(2)); % path gain between (S) and (D)for Rayleigh
fading
a1=raylrnd(1/sqrt(2)); % path gain between (S) and (R)for Rayleigh
fading
a2=raylrnd(1/sqrt(2)); % path gain between (R) and (D)for Rayleigh
fading

B1=(1^2/0.6^2); % B1 is a gain factor corresponding to the distance
between (S) and (R)
B2=(1^2/0.6^2); % B2 is a gain factor corresponding to the distance
between (R) and (D)

f=0.5*(exp(-1*((P(1)*a0^2)+(B2*P(3)*a2^2))*Ns) + exp(-
1*((P(1)*a0^2)+(B1*P(2)*a1^2))*Ns) - exp(-
1*((P(1)*a0^2)+(B1*P(2)*a1^2)+(B2*P(3)*a2^2))*Ns)); % Eq.(10) with Q=2
```